Developing a low cost multipurpose X-band FMICW radar

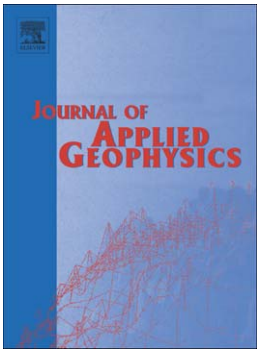

Waterborne and on-land electrical surveys to suggest the geological evolution of a glacial lake in NW Italy

Chiara Colombero, Cesare Comina, Franco Gianotti, Luigi Sambuelli

PII: S0926-9851(14)00089-5
DOI: doi: 10.1016/j.jappgeo.2014.03.020
Reference: APPGEO 2466

To appear in: *Journal of Applied Geophysics*

Received date: 17 June 2013
Revised date: 24 March 2014
Accepted date: 25 March 2014

Please cite this article as: Colombero, Chiara, Comina, Cesare, Gianotti, Franco, Sambuelli, Luigi, Waterborne and on-land electrical surveys to suggest the geological evolution of a glacial lake in NW Italy, *Journal of Applied Geophysics* (2014), doi: 10.1016/j.jappgeo.2014.03.020

Title:

WATERBORNE AND ON-LAND ELECTRICAL SURVEYS TO SUGGEST THE GEOLOGICAL EVOLUTION OF A GLACIAL LAKE IN NW ITALY.

Running Title:

ELECTRICAL SURVEYS OVER A GLACIAL LAKE.

Authors:

Chiara Colombero[1], Cesare Comina[1], Franco Gianotti[1] and Luigi Sambuelli[2]

Authors affiliation:

[1] Dept. of Earth Science (DST), Università degli Studi di Torino, via Valperga Caluso, 35, 10125 Italy;

[2] Dept. of Environment, Land and Infrastructure Engineering (DIATI), Politecnico di Torino, corso Duca degli Abruzzi, 24, 10129 Italy;

Key points:

Extensive waterborne Continuous Vertical Electrical Soundings survey.

Laterally Constrained Inversion for the identification of the lakebed sediments.

Groundwater recharge area, reconstruction of lake basin genesis.

ABSTRACT

Geophysical surveys on and around the Candia Lake, located NE of Turin (NW Italy), in the internal depression of the Ivrea Morainic Amphitheatre (IMA) right frontal sector, are reported in this paper. The surveys were intended to obtain a geophysical characterization of the lakebed, to investigate the interconnection paths between surface water and groundwater and to be used as a first general survey for suggesting the geological processes which lead to the actual morphology.

An extensive waterborne Continuous Vertical Electrical Soundings (CVES) survey consisting of 15 profiles, with a total length of about 19 km of acquisition, was carried out on the lake surface. The processing of the acquired profiles with a Laterally Constrained Inversion (LCI) approach lead to the reconstruction of the lakebed sediments distribution, down to 10 meters depth. Self Potential (SP) data recorded on the lake surface have also been analyzed. Moreover, to verify the areal distribution of the deposits, three Electrical Resistivity Tomographies (ERT) were carried out on land near the northern and southern shore of the lake. The combination of the geophysical surveys results with hydrogeological information and geological observations and interpretations allowed the characterization of the submerged deposits, the probable identification of the main areas of groundwater recharge and the preliminary reconstruction of the lake genesis.

1. INTRODUCTION

The geological characterization of the bottom sediments of a lake is essential to determine the hydrogeological properties of the deposits and to investigate the interconnecting relationship between surface water and groundwater. However, geological analysis in water-covered areas is difficult and expensive with traditional survey techniques. Direct investigations (e.g. logs or cores) are often neither cost-effective nor reasonably quick and adequate in number to cover the whole surface of a basin and to obtain a reliable correlation of data over a wide area.

Geophysical methods can therefore be very useful to investigate sediments which are entirely located beneath a water-covered area. They can be indeed profitably used not only as a validation of the results of direct techniques, but also as a tool for planning future surveys. Among the available geophysical methods the use of non-seismic methods to study shallow inland water is relatively recent. A review of the existing methods and case histories can be found in the Special Issue of Near Surface Geophysics on Waterborne Geophysics [Sambuelli and Butler, 2009; Butler, 2009].

Among the electrical techniques used for waterborne surveys, Continuous Vertical Electrical Soundings (CVES) have gained greater attention. The possibility of using multichannel resistivity meters makes it possible to simultaneously perform several resistivity measurements, in a fast and cost-effective way. CVES have been applied in water-covered areas for different purposes and using different electrode configurations. In this respect there is a wide scientific literature. Bradbury and Taylor [1984] used the CVES acquisitions with floating electrodes, together with seismic

refraction profiles, to study the hydrogeological properties of the bottom sediments of Lake Michigan (USA). Loke and Lane [2004] examined three different acquisition strategies in an aquatic environment. Their study found that the presence of a water layer between electrodes and sediments reduces the depth of investigation. Kwon et al. [2004] compared acquisitions from floating and water bottom electrodes, in order to find both the minimum electrode spacing and the thickness of the water layer allowing for the best results using different electrode configurations. Allen and Merrick [2007], in a study focused on the inversion of geoelectric data for hydrogeological purposes, demonstrated that using a floating array with exponentially spaced potential electrodes provides the maximum resolution with depth. Mitchell et al. [2008], with a combination of stationary and towed electrodes floating on the lake surface, used continuous resistivity profiling to identify heterogeneities which control seepage at Mirror Lake (USA). Another case study with hydrogeological purposes is reported in Kelly et al. [2009]. The authors investigated the capability of towed electrical cable to map a known aquifer recharge zone and to provide hydrogeological information and electrical properties of the sediments. Befus et al. [2012] carried out some resistivity profiles to delineate groundwater-lake interactions with floating equi-spaced electrodes. Geological characterization of sediments can be deduced from electrical measures as demonstrated by Rucker et al. [2011] carrying out an electrical continuous survey with floating electrodes set on a cable dragged by a boat through the whole length of the Panama Canal. Such data have been used to detail the geological mapping of the region in submerged areas to support the project of dredging and widening of the canal. All of

these previous studies agree that submerged electrodes allow better penetration in the lakebed sediments, while the selection of the electrode array is closely related to the purposes of the survey (i.e. depth of investigation and resolution required), in this respect an optimum a-priori choice does not exist. However, the use of floating electrodes seems preferable, since it is faster and less expensive than submerged ones from the acquisition point of view. With the floating cable arrangement, exponentially spaced electrodes appear to provide the best resolution with depth.

Most of multichannel resistivity meters also allow for a contemporary acquisition of Self Potential (SP) data; these could be potentially related to water paths since it is known that, roughly, water sources generate positive SP anomalies and the opposite occurs with water sinks. Recent literature works have underlined the potentiality of the SP method from waterborne acquisition for mapping groundwater-surfacewater exchanges [Grangeia and Matias, 2012]. Ishido and Pritchett [1999] carried out numerical simulation of electrokinetic potentials associated with subsurface fluid flow, using SP data which have actually been observed in real geothermal fields. They demonstrated that a positive self-potential anomaly is present above the upflow region while large negative anomalies appear in the peripheral areas where meteoric water flows downward. Goto et al. [2012] analyzed the implications of self-potential distribution caused by groundwater flow in a mountain slope. They observed positive SP anomalies related to local springs and SP decreasing pattern mainly related to vertical infiltration flow in the slope body. Other examples of studies that confirm these

correlations between water flow and SP anomalies can be found in Tique et al. [2002] and Thompson et al. [2012].

We discuss the results of a survey conducted with the CVES method on the Candia Lake, located NE of Turin (NW Italy). The main objective of the study was to obtain a first assessment on the characterization of the sediments of the basin, in order to define nature, composition, geometry and spatial relationships of the detected geological bodies for further direct investigations and for suggesting a preliminar basin genesis reconstruction. Using a Laterally Constrained Inversion (LCI) approach for the data inversion, we managed to obtain 15 resistivity sections that cover almost the entire area of the lake. By joining these profiles it was then possible to produce a three-dimensional model of the electrical resistivity distribution below the water basin. To verify the results of CVES data, two electrical on-land tomographies were also carried out on the northern shore of the lake and an additional one was performed on the southern bank. These supplementary surveys allowed extending the depth and the area of investigation of the previous method, in order to obtain a better correlation of data below the submerged area and a first order geological reconstruction based also on field evidences. Another aim of the study was to try to understand the hydrogeological dynamics that govern the lake basin, by identifying, at least qualitatively, the presence of interconnection paths between surface water and groundwater in order to localize areas in which recharge or seepage flows are concentrated. To this purpose we also analyzed the Self Potential (SP) data automatically collected on the lake surface during CVES acquisition. Since in the studied area there is no (or very scarce) availability of direct surveys (e.g. logs or cores),

we have tried to obtain as much information as possible from the combined geophysical-geological surveys. Geological analyses have been based on the stratigraphic setting of the Ivrea Morainic Amphitheatre (IMA) frontal sector, on previous studies on the Candia Lake and on specific geological surveys. The geological reconstruction finally suggested is thus to be intended as a possible interpretation and as a tool for planning and locating future direct investigations.

2. GEOGRAPHICAL AND GEOLOGICAL CONTEXT

The Candia Lake (45° 19' N, 7° 54' E) is located in north-western Italy, about 40 km NE of the city of Turin, in the Candia Canavese municipality, at an altitude of 226 m above sea level (Fig. 1). It lies on a fluvial terrace 4-8 m high above the present Dora Baltea River alluvial plain, in the frontal sector of the Ivrea Morainic Amphitheatre (IMA), between its terminal moraines and the internal plain.

The IMA is the third largest morainic amphitheatre in Italy, with 505 km^2 of extension. It is characterized by a wide flat internal depression (200 km^2) encircled by a large moraine complex (> 300 km^2) that was built by the Dora Baltea Glacier during successive glacial events which took place from the end of Early Pleistocene to the end of Late Pleistocene (900-20 ka BP). The lake basin remained owing to the glacier withdrawal from its maximum expansion during the Last Glacial Maximum (LGM). Large volumes of water released from the retreating ice mass were collected into a depression of the proglacial plain closely to the frontal moraine hills (Fig. 1).

The lake has an elongated shape in NE-SW direction, with an area of 1.5 km^2, a 5.8 km long perimeter, an average depth of about 4.7 m and a maximum depth, in the north-eastern sector, of 7.5 m, for an estimated water volume of about 7.2 Mm^3. The catchment area (about 8.9 km^2 wide) belongs to the drainage basin of the Dora Baltea River that flows across the internal plain and leaves the amphitheatre through the Mazzé gorge 5 km SE. The lake has no influent so that the water recharge can be considered to be supplied from groundwater and direct rainfalls on the catchment area as also underlined by Ciampittiello et al. [2004]. Only a small stream, Rio Traversaro, outflows from the north-western edge of the lake and flows towards the Dora Baltea River (Fig. 1). The lake is bordered on the south by the morainic hills of the right front side of the IMA, surrounding its perimeter from W to SE. These are mainly constituted by glacigenic deposits referable to the Piverone Alloformation (Late Pleistocene) and to the Serra Alloformation (end of Middle Pleistocene) described in Gianotti et al. [2008]. These two units are made up of marginal and subglacial tills, forming the frontal moraines, with overlapping marginal and proglacial glaciolacustrine deposits, especially forming kame terraces (Fig. 2). The glacial deposits show a wide range of variability, but they mostly consist of over-consolidated silty fine sands with rare clasts and subordinate coarse sand bodies with gravel.

The moraines immediately south of the Candia Lake have a ENE-WSW trending, i.e. parallel to lake basin. Only one of the more internal moraines, very close to the lake, has a NW-SE trending, i.e. perpendicular to the lake basin. This moraine aligns with a slight narrowing of the lake in the middle part of its southern shore (a in Fig. 2).

Some wide terraced plains, corresponding to kame terraces, are distributed at 250-230 m altitude between the Piverone Alloformation moraines and the Candia Lake. They are constituted by glaciolacustrine laminated silts and sands deposited into small glacial margin lakes during the slow withdrawal of the glacier front. The plain to the north of the lake is instead constituted by glaciofluvial clast-supported coarse sandy gravels.

3. DATA ACQUISITION

On 15 October 2011, following a preliminary survey reported in Sambuelli et al. [2011], 15 CVES waterborne profiles were acquired on the Candia Lake (ten of which running parallel to the NE-SW elongation of the lake and five crosswise), for a total length of approximately 19 km of acquisitions (Fig. 3a). An array of nine electrodes fixed on a floating cable dragged by a small boat was used for the survey. The choice of a floating cable was mainly due to the feasibility of the survey: the *Trapa natans* (Water chestnut) is indeed widely present in the lake (in 2006 about 500 tons have been removed from the lake) and doesn't allow to freely drag a cable on the bottom of the lake. The array (Fig. 3b) has two current electrodes, in the cable part closest to the boat, followed by seven potential electrodes. The current electrodes were 16 m apart, while the six couples of potential electrodes had exponentially increasing spacing. The first potential electrode was 0.5 m from the farthest current electrode. In the continuous profiling set up, dipole-dipole array data are collected measuring voltage potential differences between subsequent couples of potential electrodes given the same current

injecting dipole. The towed cable floated on the lake surface thanks to plastic floaters fixed near the electrodes that were fully submerged. The cable was kept stretched by a floating anchor fixed at its end.

We used a multichannel georesistivimeter (Syscal Pro in Sysmar upgrade – Iris Instruments) which was able to simultaneously acquire the six potential measurements. The resistivity meter was connected to a GPS device, in order to record the spatial position of the acquired data. The short current injection time (150 ms) allows recording the resistivities very quickly; the acquisition step is about 2 seconds which results, on average, in one vertical electric sounding every 3 m. Moreover, before any current injection, the instrument automatically records the self potential (SP) across the six potential dipoles.

On 25 October 2012, two electric on-land tomographies were acquired on the northern shore of the Candia Lake, (Fig. 3a). The resistivity measurements were carried out with the use of the same multichannel resistivity meter used for the acquisition of waterborne CVES and SP data.

The first tomography was realized with 72 electrodes at 1 m spacing, for a total length of 71 m (AA' in Fig. 3a). The acquisition line is oriented N-S, approximately normal to the elongation direction of the lake. The first measuring electrode was located at a distance of about 10 m from the lake shore. The small electrode spacing allowed obtaining a high lateral and vertical resolution of the data, at the expense of the investigation depth. In order to increase the investigation depth, a second electric tomography was acquired next to the previous one with larger electrode spacing (3 m),

for a total length of 357 m (BB' in Fig. 3a). The whole line was recorded by keeping 24 electrodes in place and rolling 48 electrodes to the front of the line.

On 14 September 2013 an additional tomography was acquired on the southern shore of the lake. This tomography was realized with 72 electrodes at 2 meters spacing, for a total length of 142 m, elongated approximately in N-S direction (CC' in Fig. 3a). An acquisition sequence with Wenner-Schlumberger configuration was employed for all the tomographies.

4. DATA PROCESSING AND METHODOLOGY

Having a great number of data from the CVES survey (one VES approximately every 3-4 m) we decided to evaluate mean values every 6 subsequent acquisitions in order to reduce the computational effort of the inversion. In this way we obtained 800 mean apparent resistivity curves over the whole lake, for an approximate sampling interval of 15-20 m (that corresponds also, roughly, to the current electrodes separation). Each averaged curve provides an apparent resistivity curve that is located in the centre of the considered spatial window.

Before the inversion a statistical analysis of the data was performed, in order to evaluate the homogeneity of water resistivity and data variability with depth. We calculated mean, standard deviation, median, minimum and maximum of the apparent resistivity values for each of the six dipoles for the 800 mean VES. From the results reported in Figure 4 it appears clear that the first three dipoles investigated the lake water, which has a constant value of about 85 Ωm throughout the basin. This is

highlighted also by the standard deviation bars pertaining to these three dipoles which are small compared to the mean values of the measurements.. The last three dipoles are expected to give information about the lakebed sediments. From the mean and median trends it can be inferred that most of the investigated sediments show resistivity values that are lower than water resistivity and only a small fraction of them have higher values.

From the observation of the raw data it was evident, even before the inversion, that higher resistivity values in the sediments are located in the central part of the southern shore of the lake where a strong positive anomaly is located. This can be clearly seen in the result reported in Figure 5b where the difference in the measured apparent resistivity values of the last two dipoles is plotted and interpolated, by means of triangulation with linear interpolation method, over the lake surface. It is confirmed that the investigated lake sediments show higher resistivities (positive difference among the last two dipoles) only in the southern part of the basin. In this same zone, as discussed before, there is geological evidence of a NW-SE trending internal moraine (a in Fig. 2).

After this preliminary data treatment the CVES data were inverted using a Laterally Constrained Inversion (LCI) approach. The LCI was developed to invert CVES data acquired along a profile by Auken and Christiansen [2004]. This approach is based on a pseudo-2D layered parameterization of the investigated geological medium: the inversion result is a set of 1D consecutive resistivity models, each one corresponding to a sounding, composing a pseudo-2D section. All the VES soundings along a profile are inverted simultaneously by minimizing a common objective function, which contains

all the acquired data, the available a-priori information and lateral constraints among consecutive models. The inversion scheme can be written for the *(n+1)-th* iteration as:

$$\mathbf{m}_{n+1} = \mathbf{m}_n + \left(\begin{array}{l} \left[\mathbf{G}^T \mathbf{C}_{obs}^{-1} \mathbf{G} + \mathbf{P}^T \mathbf{C}_{prior}^{-1} \mathbf{P} + \mathbf{R}^T \mathbf{C}_R^{-1} \mathbf{R} + \lambda \mathbf{I} \right]^{-1} \times \\ \left[\mathbf{G}^T \mathbf{C}_{obs}^{-1} \left(\mathbf{d}_{obs} - fw\left(\mathbf{m}_n \right) \right) + \mathbf{C}_{prior}^{-1} \left(\mathbf{m}_{prior} - \mathbf{m}_n \right) + \mathbf{R}^T \mathbf{C}_R^{-1} \left(-\mathbf{R}\mathbf{m}_n \right) \right] \end{array} \right)$$

where m is a vector including all the parameters (electrical resistivity and thickness of each layer) relative to the spatially distributed 1D resistivity models. The vector m is linked to the observed data set d_{obs} (apparent resistivity curves) through the forward modeling *fw*. The matrix R is the model parameters lateral regularization matrix and P is the one relative to the a priori information. The effectiveness of the R and P matrices depends on the strength of the constraints described in the covariance matrices C_R and C_{prior}. The problem of non-linearity is taken into account by means of the regularizing Marquart damping parameter λ. An appropriate Matlab® code has been developed to implement the inversion and the forward problem was computed with the CR1Dmod algorithm [Ingeman-Nielsen and Baumgartner, 2006] considering homogeneous horizontal layers. A similar approach has been applied in the preliminary investigations on the lake Sambuelli et al. [2011].

Through the lateral constraints, information from one vertical electrical sounding are interconnected with the neighboring ones, producing the final pseudo-2D section. The lateral constraints are chosen in a way to allow for pseudo-2D sections that are more or less homogeneous on the basis of the geological setting of the investigated area. In particular, the degree of lateral homogeneity of the considered model parameters is

controlled by the strength of the constraints contained in the C_R matrix. If the expected lateral variability is small, a strong constraint will be applied; conversely if a large variation is expected, the strength of the constraint will be relaxed.

For a reliable inversion auxiliary a-priori data are also fundamental to ensure that as much known information as possible is considered in the inversion process. Crucial information for waterborne surveys includes bathymetry and water resistivity, which describe the properties of the water column. By providing these constraints in the covariance matrix C_{prior}, the inversion procedure is focused on the deposits beneath the lake bottom, thus allowing a more accurate delineation of the sediment's electrical properties.

The conceptual reference model on which the inversion process was based is a three layered medium. For each inversion it was possible to a-priori fix the thickness (h1) and the resistivity (ρ1) of the water column (first layer). The first layer thickness h1 was a-priori known throughout the lake (Fig. 5a) from previous Ground-Penetrating Radar surveys [Sambuelli and Bava, 2011; Sambuelli et al., 2011]. The first layer resistivity ρ1 was kept constant (85 Ωm) considering the low variation of the mean of the nearest potential dipoles and the results of water electrical conductivity direct measurements, carried out in several points of the lake surface for the present study and in previous surveys [Sambuelli and Bava, 2011]. The introduction of these two a-priori information also reduced the "problem of equivalence" (Telford et al., 1990) given by the presence of a conductive layer between two layers with a higher resistivity, which is observed particularly on the southern shore (Figure 5b).

On the contrary, the second and the third electrical layers, representing the lakebed sediments, could not be considered laterally homogeneous, given the complexity of the geological context of the site. For this reason it was necessary to focus the attention on the strength of the constraints applied to these layers. To allow for an automatic selection of the constraints, these have been chosen on the basis of the lateral variability of the raw data at greater depths of investigation (Fig. 5b). As an example, the constraint on the resistivity of the third layer (ρ3), which is the most variable one, has been evaluated on the basis of the variation of the apparent resistivity between the dipoles M6 and M7 in two consecutive VES curves. The constraint is proportional to the squared inverse of the difference of $|(\rho M6\text{-}M7)_n - (\rho M6\text{-}M7)_{n+1}|$. In this way, weaker constraints are locally selected when a transition of resistivity is noted in the raw data, particularly in correspondence to the resistivity anomaly on the southern shore (Fig. 5b). The inversion of electric tomographies was performed with the Res2DInv software [Loke and Barker, 1996].

The recorded SP data were manually filtered and interpolated by means of triangulation with linear interpolation method on the whole area of the basin, in order to obtain a map of the natural potential present throughout the basin for each potential dipole.

5. RESULTS

5.1 Continuous Vertical Electric Soundings

Results obtained from LCI showed that, below the water, a relatively uniform layer of deposits characterized by resistivity values between 10 and 30 Ωm is present (in red in Fig. 6). This layer has however a variable thickness from a few decimetres to a few metres. Below this layer the lakebed doesn't show horizontally constant resistivity values. The northern sector of the basin is still characterized by deposits with resistivity values lower than water resistivity (Fig. 6a) for the whole depth of investigation (about 10 m); on the contrary, along the southern shore of the lake higher resistivity values (250-300 Ωm) are observed (in yellow in Fig. 6c). Combining the results of all fifteen profiles using a triangulation with linear interpolation method, it was possible to visualize a 3D model of the resistivity of the submerged environment (Fig. 7) which illustrates the overall setting and the observed difference between south and north sides of the lake.

5.2 On-land Electrical Resistivity Tomographies and Self-Potentials

The resistivity sections resulting from the processing of the on-land ERT enlarged the area of investigation, in order to evaluate the lateral continuity of the observed geological formations, and increased the depth of investigation on the northern shore where thicker conductive sediments limit the penetration of CVES data. Results of the three ERT performed are shown in Figure 8. The elevation of each tomographic

profile was approximately the same as the lake surface so that a comparison with CVES results (Fig. 6) is possible.

Specifically the ERT section CC' (Fig. 8a), obtained from the survey on the southern bank, has confirmed the geophysical setting resulting from the CVES data inversion in this location. Indeed the section part closest to the lake shows low resistivity deposits (10-30 Ωm) overlying sediments with resistivity values higher than lake water (up to 300 Ωm) and comparable to the ones observed in CVES inversions near the south shore (Fig. 6c).

From the shorter high-resolution section AA' acquired on the northern shore of the lake (Fig. 8c), it was possible to detect the depth of the water table, at about 80 cm below ground level in the area immediately north of the lake. Also in the north shore, the longer section BB' (Fig. 8b) shows higher resistivity deposits at depths not reached by the CVES survey in this location (greater than 10 m), although characterized by lower resistivity values (80-100 Ωm) compared to the ones observed along the southern shore of the lake (250-300 Ωm) in both the waterborne CVES survey (Fig. 6c) and from the ERT section CC' (Fig. 8a). Above these deposits the area closest to the lake is characterized by deposits with resistivity values similar to the ones detected on the bottom of the lake by the CVES survey (10-30 Ωm). Towards the north these deposits progressively pass to sediments characterized by higher resistivity both laterally (50-60 Ωm) and vertically (90-100 Ωm) on the top of the section BB'.

Finally, the SP map (Fig. 9) obtained from the M4-M5 dipole of the CVES array identifies positive anomalies near the central and western part of the southern shore. The remaining area of the lake is characterized by negative values of SP.

6. DISCUSSION

6.1 Lake bottom sediments and suggested geological reconstruction

A representative N-S cross section reporting the geophysical results and their geological interpretation is reported in Fig. 10. The waterborne CVES survey and the on-land ERT investigations allowed the stratigraphic reconstruction of the subsoil both in submerged and emerged environment. They essentially show an upper sedimentary unit with low resistivity values (10-30 Ωm) resting on a lower complex with higher resistivity (varying from about 90 to 300 Ωm).

According to the reconstructed buried morphology (presence of like-moraine reliefs), position (frontal sector of a end moraine system) and resistivity values, the electric lower complex can be interpreted as submarginal glacial deposits forming very low end moraines, whose characters are likely similar to the *lithofacies* of the moraines outcropping south of the lake (1 in Fig. 10). These low reliefs could be interpreted as kame-moraines, formed into an aquatic environment and partially made up of more sorted and permeable deltaic and glaciolacustrine deposits. The gradual decrease in the resistivity of these deposits, from south to north, may be either attributed to **i)** heterogeneities in the particle size (higher resistivity in presence of blocks, boulders and

gravels along the southern shore and finer particle size towards north) or **ii)** the variation of pore fluids characteristics, as we discuss below (see §6.3).

Concerning the upper resistivity unit below the lake, the CVES show a single sedimentary body with variable thickness (from a few decimeters to some meters) characterized by resistivity values between 10 and 30 Ωm. These values are consistent with lacustrine deposits consisting of silts and clays with organic matter (5 in Fig. 10), similar to the recent gyttja sampled by Lami et al. [2000] in the upper 100 cm from the lakebed using a gravity corer fitted with a PVC tube (1.5 m long with a diameter of 63.5 mm). This last study confirmed the clayey-silty composition and the high organic matter content (37%) of the shallower lacustrine deposits.

Nevertheless it is unlikely that the entire fill, which at some locations is quite thick, is represented only by non-glacigenic lacustrine sediments. First, the presence of buried moraines under the lake indicates a few glacier halts which would have associated sediment discharge. Second, an advancing delta (see also below) certainly supplied sediments to the distal sector of the basin, which corresponds to the present lake. Finally, if the non-glacigenic sedimentation in the Candia Lake has occurred for 25 ka BP starting from the time of the main local glacial retreat (see §6.4), the first half of this time interval occurred during LGM and Lateglacial, i.e. in a very cold climate [e.g. Ivy-Ochs et al., 2012]. According to this evidence, it seems reasonable to differentiate the filling up sequence of the present lake into three levels (Fig. 10): a lower level, consisting of glaciolacustrine sands and silts corresponding to delta bottomset sediments (2); an intermediate level, consisting of non-organic lacustrine fine sediments (5a)

deposited into a non-glacial lake, very similar to the present lake, but still in a glacial climate (25-16 ka BP); and an upper level, consisting of organic-rich lacustrine sediments (5b) deposited into a basin surrounded by wooded banks due to a warmer climate (16-12.7 ka BP and from 11.6 ka, i.e. in the Holocene; Vescovi et al., 2007; Ravazzi et al., 2012). Due to the similar texture of the deposits indicated with numbers 2 and 5 in Figure 10 it was not possible to distinguish them from a geophysical point of view since they have the same resistivity range (10-30 Ωm).

The sedimentation rates of similar (small and without tributary streams) lake basins can be taken into account to establish a reasonable thickness of the post-glacial lacustrine deposits. As a reference, we consider the 28 m thick Fimon lacustrine succession, filling a non-glacial lake in the Colli Berici Hills (NE Italy). Filling started 140 ka BP, suggesting an average sedimentation rate of 0.2 mm/yr (0.7 mm/y if we consider the upper 19.4 m of the core, starting from 27 ka BP) [Pini et al., 2010]. Sedimentation rates between 0.3 mm/yr (in the last millennium) and 2 mm/yr (in the modern period) were obtained for the sediments of the Candia Lake [Lami et al., 2000]. Using a sedimentation rate of 0.2 mm/yr, a 5 m thickness of nonglacigenic lacustrine deposits is obtained for the Candia Lake starting from 25 ka BP, which is the time of the ice-dammed lake death caused by the glacial retreat.

North of the actual lake these low resistivity deposits rapidly transit laterally to sediments with higher resistivity values (40-60 Ωm, 3 in Fig. 10). The overall subsoil geometry and the flat surface morphology of this side of the lake, which consists of outcropping fluvial gravels (4a in Fig. 10) and not of palustrine deposits at the surface,

can be explained by hypothesizing a previous wider ice-dammed lake filled up by an advancing delta. The northern part of this lake was indeed probably quickly filled by a Pleistocene delta-fan sequence constituted by silty sands, interpretable as turbiditic bottomset deposits (2 in Fig. 10), followed by gravelly sands interpreted as foreset deposits (3 in Fig. 10). The lacustrine sequence was only finally covered by coarse clast-supported sandy gravels of glaciofluvial origin constituting the topset unit of the sequence (4 in Fig. 10) and corresponding to the upper resistivity unit in the plain sector.

This sequence is quite typical of a Gilbert-type delta [Gilbert, 1890]. In absence of outcrops or core data it is not possible to distinguish if the delta is of glacial marginal position (Gilbert-type ice-contact delta) [Feenstra et al., 1988; Lønne, 1993] or it is of proglacial position (Gilbert-type glaciofluvial delta) [Lønne, 1995; Benn and Evans, 1998; Kostic et al., 2005].

6.2 Hydrogeological aspects

From a hydrogeological point of view, the self-potential map shows negative values over almost the whole area of the lake while some positive anomalies are localized near the southern shore of the lake. These positive SP anomalies could therefore be preliminary interpreted as related to the main underwater recharge areas of the lake. Groundwater discharge is the major water source of the lake basin, as deduced from the hydrological balance of the lake [Ciampittiello et al., 2004]. Moreover, SP anomalies are correlated with other geophysical and geological evidence consistent with localized groundwater discharge. Particularly in the same area where positive SP

anomalies are located the CVES results show glacigenic deposits closer to the lake bottom overlain by a thin mantle of lacustrine silts, thus facilitating groundwater discharge. On the other hand, negative anomalies may indicate a weak process of infiltration of the lake water into the lacustrine silts that slowly recharges the groundwater of the plain to the north.

6.3 Consideration about the water resistivity

During the surveys, a strong resistivity contrast between lake water and groundwater in the north of the basin was observed. The lake water has a resistivity of about 85 Ωm, while groundwater resistivity, measured in Cascine Rossi water-well (about 500 m north of the lake, Fig. 2 and 3a), has a value around 19 Ωm. The well water analysis shows a Total Dissolved Solids (TDS) value of about 500 mg/l.

This resistivity contrast can be explained by the hydrogeological context of the lake. Electrical resistivity and TDS are indeed negatively correlated because the conduction of current in an electrolyte solution primarily depends on the concentration of ions. In addition, resistivity is also dependent on temperature. As a result, TDS values (S [ppm]) may be transformed to corresponding resistivity value (ρ_{25} [Ωm]) at a standard temperature of 25°C [Wagner et al., 2006]:

$$\rho_{25} = 2992.1 S^{-0.925} \qquad (2).$$

To estimate the resistivity at another temperature (ρ_T) some experimental correlations between water conductivity and temperature must be performed [Hayashi, 2004]:

$$\rho_T = \frac{\rho_{25}}{1+0.02(T-25)} \qquad (3).$$

We found that the difference in resistivity in the glacigenic deposits under the lacustrine sediments (1 in Fig. 10) is consistent with an increasing salt content from south to north. The lake water is indeed a mixture of direct rainwater on the lake, runoff and water infiltrated through the hills just south of the lake. This water flows along quite short paths in the morainic materials before reaching the lake and does not have time enough to get rich in salts. Considering an hypothetical initial TDS of 70 mg/l, we obtained a water lake resistivity of 79 Ωm, in agreement with the CVES measurements (85 Ωm). We then hypothesized that this initial value could rise up to 150 mg/l within the sediments near the south bank of the lake and we obtained a water resistivity of 39 Ωm. Using Archie's formula [Archie, 1942]:

$$\rho_F = a\frac{\rho_w}{\varphi^m} \qquad (4)$$

where ρ_F is the formation resistivity, ρ_w is the water resistivity, a =1 and m=1.4 are Archie's coefficients for non-consolidated sediments [Friedman, 2005], φ is the porosity that, based on literature data for similar deposits [Tu et al., 2013], can be set to 0.23. We obtained a formation resistivity of 305 Ωm, close to the one obtained by CVES (250-300 Ωm in Fig. 6c and Fig. 10). Continuing the hypothesis of a salt enrichment going north,

we then calculated the resistivity of a water with TDS equal to 500 mg/l, as measured at the Cascine Rossi borehole, and we obtained 12.9 Ωm, resulting in a formation resistivity equal to 101 Ωm comparable to the one (70-90 Ωm) of the deepest formation obtained from BB' tomography in the northern bank of the lake (Fig. 8b and Fig. 10).

Therefore, these considerations, the geological environment and the small correlation distance allow considering that the deepest formation observed during electrical surveys has mainly the same geologic composition even if with different saturating water properties. Only partially, on the northern shore, this formation could be made up of more sorted and permeable deltaic and glaciolacustrine deposits and this will give a further increase in the overall resistivity and its permeability as evidenced by SP surveys and the ERT section on the north shore (Fig. 8a and Fig. 10).

6.4 Geological evolution of the area suggested by geophysical tests.

Based on the study results, a preliminary reconstruction of the geological evolution of the area is proposed (Fig. 11). This reconstruction is also based on a stratigraphical model of the glacial margin sedimentary system which derives from a wide literary source [e.g. Bennett and Glasser, 2009; Evans et al., 2012], makes use of the international classification of glacigenic deposits [Goldthwait and Matsch, 1989] and was verified and adjusted by means of specific geological surveys in the IMA [Gianotti, 2007; Gianotti et al., 2008].

The frontal moraines forming the reliefs south of the Candia Lake (Fig. 11a) are genetically linked to the maximum expansion of the Dora Baltea Glacier in the last

glacial cycle (Piverone Alloformation, local LGM, likely in MIS2) [Gianotti et al., 2008], correlated to the first phase of glacial advance in the Tagliamento Amphitheatre (NE Italy) during the LGM, dated at 26.5-23 cal. ka BP [Monegato et al., 2007].

With a first moderate withdrawal of the glacier front, the melt-out water from the retreating glacier was at first discharged into ephemeral glacial marginal lakes, strictly confined between the moraines and the glacier front. Their sedimentary filling formed sub-horizontal planes suspended on the inner flank of the moraines, named kame terraces (Fig. 11b). They develops just from the morainic crests, where sporadic small planes are preserved, to the foot of the moraines, where larger terraces are suspended only some meters above the Candia lake and the alluvial plain (Fig. 2).

When the mass balance of the glacier became negative because of a climatic change, the glacial margin retreated in response to an equilibrium line altitude rising [see Oerlemans et al., 2011]. A total separation of the glacier from its terminal moraines was finally obtained (Fig. 11c). The residual melt-out waters were hosted into a subglacial genesis depression remained at the foot of the frontal morainic reliefs, to give rise to the early proglacial Candia Lake.

The geophysical outcomes suggest that the proximal (northern) sector of a glaciolacustrine basin wider than the present lake was filled by an advancing delta, directly fed from the glacier meltwaters. The preservation of the lake itself supports the hypothesis of a glaciolacustrine delta: the basin was not completely filled because the fast glacigenic sedimentation stopped suddenly due a more pronounced retreat of the glacier. A very slower lacustrine sedimentation continued into the relict basin. This

event can be referred to the middle LGM, about 25-23 ka BP, i.e. before the building of the Ivrea Alloformation end moraines [Gianotti et al., 2008] 5 km upstreams.

7. CONCLUSIONS

The interpretation of waterborne methods (CVES, SP) and on-land surveys (ERT) on and around the Candia Lake suggested a geological reconstruction that reflects the typical conditions of a glacigenic sedimentary system evolving from a marginal to a proximal proglacial environment. The geophysical surveys were supported by surface data obtained through geological observations on the relief around the lake. The results were compared with a stratigraphical model of the glacial margin sedimentary system suitable for the frontal sector of the IMA. The reconstructed stratigraphy allowed to preliminary explain the lake basin genesis as a former wider basin gradually but quickly filled in by an advancing fluvio-lacustrine delta in a marginal evolving to proglacial environment during the last glaciation.

The underwater discharge is the largest water supply to the lake. The main hydrogeological window connecting surface and underground water can be likely identified in the glacial marginal deposits constituted of silty sands with gravel bodies. These deposits largely outcrops as kame terraces on the reliefs south of the lake, while in the lake bottom they are part of kame-moraines. The SP method seems to preliminary locate the main discharge areas in the central and western part of the southern shore, where these deposits appears, also from the other geophysical tests, to be closer to the

bottom of the lake and lacustrine silts have reduced thickness. These sites can reasonably be considered the preferential ways for the underwater recharge.

The case study has highlighted the potential of the CVES technique as a first draft survey for determining the stratigraphical setting of an underwater environment, through the use of floating electrodes pulled by a boat. The presence of a water layer of modest thickness, about 5 m on average, although limiting the depth of investigation, has allowed the reconstruction of the spatial distribution of resistivity in the submerged deposits down to approximately 10 m with the adopted array. The accuracy and resolution of CVES data interpretation are improved when the data inversion is constrained by bathymetry and water resistivity values. The CVES methodology has still some limitations: the depth of investigation is contained and, while working in a complex geological context, it is necessary to focus the attention on the strength of constraints for the inversion processing. In addition, since it is an electrical technique, it should be noted that resistivity does not have unique and diagnostic values for each lithology. Geological conclusions are therefore based on possible interpretations, depending on the stratigraphical, hydrological and structural context in which we worked.

However, one of the advantages of the method highlighted by the study is the ability to cover wide areas in a quick and economically sustainable way. Moreover, even if direct surveys are not available especially for the deepest formation, it is possible to set a reference geological model for the data inversion and to obtain sounding results thanks to a-priori information.

ACKNOWLEDGMENTS

The authors would like to thank the "Ente Parco naturale di interesse provinciale del Lago di Candia" for the permission to work on the lake and publish the results. Thanks are also due to Diego Franco for his fundamental help in collecting field data. Many thanks also to one anonymous reviewer for his detailed and helpful work in the review process which helped strongly to improve the paper quality.

REFERENCES

Allen, D., and N. Merrick (2007), Robust 1D inversion of large towed geo-electric array datasets used for hydrogeological studies, Exploration Geophysics (Collingwood, Australia), 38, 50-59.

Archie, G. E. (1942), The electrical resistivity log as an aid in determining some reservoir characteristics, Transactions of the American Institute of Mechanical Engineers, 146, 54–67.

Auken, E., and A. V. Christiansen (2004), Layered and laterally constrained 2D inversion of resistivity data, Geophysics, 69, 752-761.

Benn, D. I., and D. J. A. Evans (1998), Glaciers and glaciations, Arnold, London.

Bennett, M. R and N. F. Glasser (2009). Glacial Geology. Ice sheets and landforms. John Wiley & Sons, Chichester.

Bradbury, K. R., and R. W. Taylor (1984), Determination of the hydrogeological properties of lakebeds using offshore geophysical surveys, Ground Water, 22, 690-695.

Befus K. M., Cardenas M. B., Ong J. B. and V. A. Zlotnik (2012), Classification and delineation of groundwater-lake interactions in the Nebraska Sand Hills (USA) using electrical resistivity patterns, Hydrogeology Journal, 20, 1483-1495.

Butler, K. E. (2009), Trends in waterborne electrical and EM induction methods for high resolution sub-bottom imaging, Near surface Geophysics, 7, 241-246.

Ciampittiello, M., G. Galanti, G. Giussani, I. Cerutti, A. Pranzo, F. Salerno, G. Tartari, and G. Tartari (2004), Progetto MI.CA.RI., Strumenti e procedure per il miglioramento della capacità ricettiva di corpi idrici superficiali. Attività A1. Definizione di metodologie per la valutazione dei carichi in corpi idrici superficiali: Lago di Candia, Report CNR-ISE 02.04, Istituto per lo Studio degli Ecosistemi, CNR, Verbania Pallanza, 17 pp.

Evans, D. J.A., Hiemstra, J. F., Boston, C. M., Leighton, I., Cofaigh, C. Ó. and B. R. Rea (2012), Till stratigraphy and sedimentology at the margins of terrestrially terminating ice streams: case study of the western Canadian prairies and high plains, Quaternary Science Reviews, 46, 80-125.

Feenstra, B. H., and J. Z. Frazer (1988), Fonthill kame-delta, in: Barnett, P.J. and R. I. Kelly (Eds.), Quaternary History of Southern Ontario, INQUA, XII Congress Guidebook A11.

Friedman S. P. (2005), Soil properties influencing apparent electrical conductivity: a review, Computers and electronics in agriculture, 46, 45-70.

Gianotti, F. (2007), Stratigrafia dell'Anfiteatro Morenico di Ivrea, PhD Thesis, unpublished, Università degli Studi di Torino, 270 pp.

Gianotti, F., M. G. Forno, S. Ivy-ochs and P. W. Kubik (2008), New chronological and stratigraphical data on the Ivrea amphitheatre (Piedmont, NW Italy), Quaternary International, 190, 123-135.

Gilbert, G.K. (1890), Lake Bonneville, U.S. Geol. Surv. Monograph 1, 438 pp.

Goldthwait, R.P., and C. L. Matsch (1989), Genetic Classification of Glacigenic Deposits, Taylor and Francis, Balkema, Rotterdam, 304 pp.

Goto, T., K., K. Kondo, R. Ito, K. Esaki, Y. Oouchi, Y. Abe, and M. Tsujimura (2012), Implications of Self-Potential Distribution for Groundwater Flow System in a Nonvolcanic Mountain Slope, International Journal of Geophysics, Article ID 640250, 10 pp., doi:10.1155/2012/640250

Grangeia, C., and M. Matias (2012), Shallow Water Integrated Geophysical Survey - A Case Study with Geological and Hydrogeological Consequences, Near Surface Geoscience 2012, 18th European Meeting of Environmental and Engineering Geophysics, Paris, France.

Hayashi, M. (2004), Temperature-electrical conductivity relation of water for environmental monitoring and geophysical data inversion, Environmental Monitoring and Assessment, 96, 119-128.

Ingeman-Nielsen, T., and F. Baumgartner (2006), CR1Dmod: A matlab program to model 1D complex resistivity effects in electrical and electromagnetic surveys, Computers & Geosciences, 9 (32), 1411–1419.

Ishido, T., and J. W. Pritchett (1999), Numerical simulation of electrokinetic potentials associated with subsurface fluid flow, Journal of Geophysical Research, 104, 247-259.

Ivy-Ochs, S., Kerschner, H., Reuther, A., Preusser, F., Heine, K., Maisch, M., Kubik P.W. and C. Schlüchter (2008), Chronology of the last glacial cycle in the European Alps, Journal of Quaternary Science, 23, 559–573.

Kelly, B. F. J., D. Allen, K. Ye, and T. Dahlin (2009), Continuous electrical imaging for mapping aquifer recharge along reaches of the Namoi River in Australia: Near Surface Geophysics, 7 (4), 259-270.

Kostic, B., A. Becht, and A. Thomas (2005), 3-D sedimentary architecture of a Quaternary gravel delta (SW-Germany): Implications for hydrostratigraphy, Sedimentary Geology, 181, 143-171.

Kwon, H. S., J. H. Kim, H. Y. Ahn, J. S. Yoon, K. S. Kim, C. K. Jung, S. B. Lee, and T. Uchida (2005), Delineation of a fault zone beneath a riverbed by an electrical resistivity survey using a floating streamer cable, Exploration Geophysics, Collingwood, Australia, 36, 50-58.

Lami, A., A. Marchetto, R. Lo Bianco, P. G. Appleby and P. Guilizzoni (2000), The last ca2000 years paleolimnology of Lake Candia (N. Italy) : inorganic geochemistry, fossil pigment sand temperature time-series analyses, J. Limnol., 59 (1), 3-46.

Loke, M. H., and R. D. Barker (1996), Rapid least-squares inversion of apparent resistivity pseudosections using a quasi-Newton method, Geophys. Prospect., 44, 131-152.

Loke, M. H., and J. W. Lane (2004), Inversion of data from electrical resistivity imaging surveys in water-covered areas, Exploration Geophysics (Collingwood, Australia), 35 (4), 266-271.

Lønne, I. (1995), Sedimentary facies and depositional architecture of ice-contact glaciomarine systems, Sediment. Geol., 98, 13-43.

Mitchell, N., J. E. Nyquist, L. Toran, D. O. Rosenberry and J. S. Mikochik (2008), Electrical resistivity as a tool for identifying geologic heterogeneities which control seepage at Mirror Lake, SAGEEP 2008, 11.

Oerlemans, J., Jania, J. and L. Kolondra (2011), Application of a minimal glacier model to Hansbreen, Svalbard, The Cryosphere, 5, 1-11.

Pini, R., C. Ravazzi and P. J. Reimer (2010), The vegetation and climate history of the last glacial cycle in a new pollen record from Lake Fimon (southern Alpine foreland, N-Italy), Quaternary Science Reviews, 29, 3115–3137.

Ravazzi, C., Badino, F., Marsetti, D., Patera, G. and P. J. Reimer (2012), Glacial to paraglacial history and forest recovery in the Oglio glacier system (Italian Alps) between 26 and 15 ka cal BP, Quaternary Science Reviews, 58, 146-161.

Rucker, D. F., G. E. Noonan and W. J. Greenwood (2011), Electrical resistivity in support of geological mapping along the Panama Canal, Engineering Geology, 117 (1-2), 121-133.

Sambuelli, L., and K. E. Butler (2009), Foreword, in: Special Issue on High Resolution Geophysics for Shallow Water, Near surface Geophysics, 7, 3-4.

Sambuelli, L., C. Comina, S. Bava and C. Piatti (2011), Magnetic, electrical, and GPR waterborne surveys of moraine deposits beneath a lake: a case history from Turin, Italy, Geophysics, 76, 1-12.

Sambuelli, L., and S. Bava (2011), Case study: A GPR survey on a morainic lake in northern Italy for bathymetry, water volume and sediment characterization, Journal Of Applied Geophysics, 81, 48-56.

Telford, W. M., L. P. Geldart, and R. E. Sheriff (1990), Applied Geophysics, Cambridge University Press, 770 pp.

Thompson, S., B. Kulessa, and A. Luckman (2012), Integrated electrical resistivity tomography (ERT) and self-potential (SP) techniques for assessing hydrological processes within glacial lake moraine dams, Journal of Glaciology, 58 (211), 849-858, doi: 10.3189/2012JoG11J235

Trique, M., F. Perrier, T. Froidefond, J.-P. Avouac, and S. Hautot (2002), Fluid flow near reservoir lakes inferred from the spatial and temporal analysis of the electric potential, J. Geophys. Res., 107 (B10), 2239, doi:10.1029/2001JB000482.

Tu, G., R. Huang, H. Deng and Y. Li (2013), Permeability and sedimentation characteristics of Pleistocene fluvio-glacial deposits in the Dadu river valley. Southwest China, Journal of Mountain Science, 10, 482-493.

Vescovi, E., Ravazzi, C., Arpenti, A., Finsinger, W., Pini, R., Valsecchi, V., Wick, L., Ammann, B., and W. Tinner (2007), Interactions between climate and vegetation on the southern side of the Alps and adjacent areas during the Late-glacial period as recorded by lake and mire sediment archives, Quaternary Science Reviews, 26, 1650-1669.

Wagner, R. J., R. W. Boulger Jr., C. J. Oblinger and B. A. Smith (2006), Guidelines and Standard Procedures for Continuous Water-Quality Monitors: Station Operation, Record Computation, and Data Reporting, U.S. Geological Survey Techniques and Methods 1-D3, 51 pp.

FIGURE CAPTIONS

Figure 1. *Digital Terrain Model of the Ivrea Morainic Amphitheatre (IMA) (a) at the Dora Baltea Valley outlet (b), where the study area develops (white box). Candia Lake (c) and the Viverone Lake (d) fill up two depressions on high terraces of the internal plain (e). The remarkable 16 km long Serra d'Ivrea moraine (f) in the left lateral sector. The Colli d'Ivrea abrasion reliefs (g) and the outer outwash (proglacial) plain (h) are pointed out too. The Candia Lake location and the considerable difference in altitude between the internal and the outer fluvioglacial plains are shown in the bottom topographical profile (white trace in the map).*

Figure 2. *Geological sketch of the study area with evidence of on-land ERT performed.*

Figure 3. *(a) Surveys performed. The ciano lines on the water surface refer to the fifteen CVES profiles acquired. The yellow, orange and green profiles inversions will be shown in Figure 6. The black lines on the northern and the southern shores of the lake are instead related to the three on-land tomographies. (b) Sketch of the adopted cable geometry.*

Figure 4. *Statistical analysis on raw data (800 mean apparent resistivity curves); the error bars correspond to $\pm 1\sigma(\rho_{app})$. Dipole number 1 is the potential couple nearest to the boat (M1-M2 in Figure 3b); dipole number 6 is the farthest (M6-M7 in Figure 3b).*

Figure 5. *(a) Bathymetry map of the Candia Lake obtained from the previous GPR survey of Sambuelli and Bava (2011). (b) Map of the apparent resistivity difference among the two last measuring dipoles (M5-M6 and M6-M7 in Figure 3b). The green dashed lines refer to the 15 acquired profiles, from which the data were interpolated.*

Figure 6. *Examples of LCI inversion of three CVES profiles obtained with variable lateral constraints, fixed water resistivity and bathymetry: along (a) the northern shore (green profile in Figure 3a), (b) the central part (orange profile in Figure 3a) and (c) the southern shore (yellow profile in Figure 3a) of the lake.*

Figure 7. *Horizontal slices of the bottom sediments obtained from the three-dimensional reconstruction and interpolation of the LCI results.*

Figure 8. *On-land electric tomographies: (a) CC' on the southern shore and (b) BB' on the northern shore of the Candia Lake. The dashed contoured area in BB' profile roughly overlaps the section below AA' profile (c).*

Figure 9. *Self Potential (SP) map on the Candia Lake.*

Figure 10. *Geological cross-section of the Candia Lake area derived from the geophysical surveys (reported on top of the figure). The hilly morphology of the deepest resistivity boundary suggests the presence of buried forming moraines submarginal till (1). The extension of fine glaciolacustrine deposits (2 and 3) both under the lake and the plain suggests the wider extent of a former lake. This reconstruction explains the Candia lake genesis as the relict of a wider ice-damned lake, not completely filled up by deltaic deposits coming from the glacier. The filling up of the lake very much slackened with the complete retreat of the glacier (5a) and continued till now (5b) owing to a moderate colluvial and alluvial supply (6) from the southern side of the basin.*

Figure 11. Suggested r*econstruction of the glacial margin stadial events (T1-T5) in the front side of the IMA during the LGM. A frontal moraine is built during a main glacial margin stationary phase with tendency to expansion (a). Kame terraces form on the moraine internal side during a subsequent first slow glacier withdrawal interrupted by brief stops (b). Lower submerged kame-moraines are built in the internal depression during temporary halts of the retreating glacier front at the edge of a progressively wider ice-dammed lake (c).*

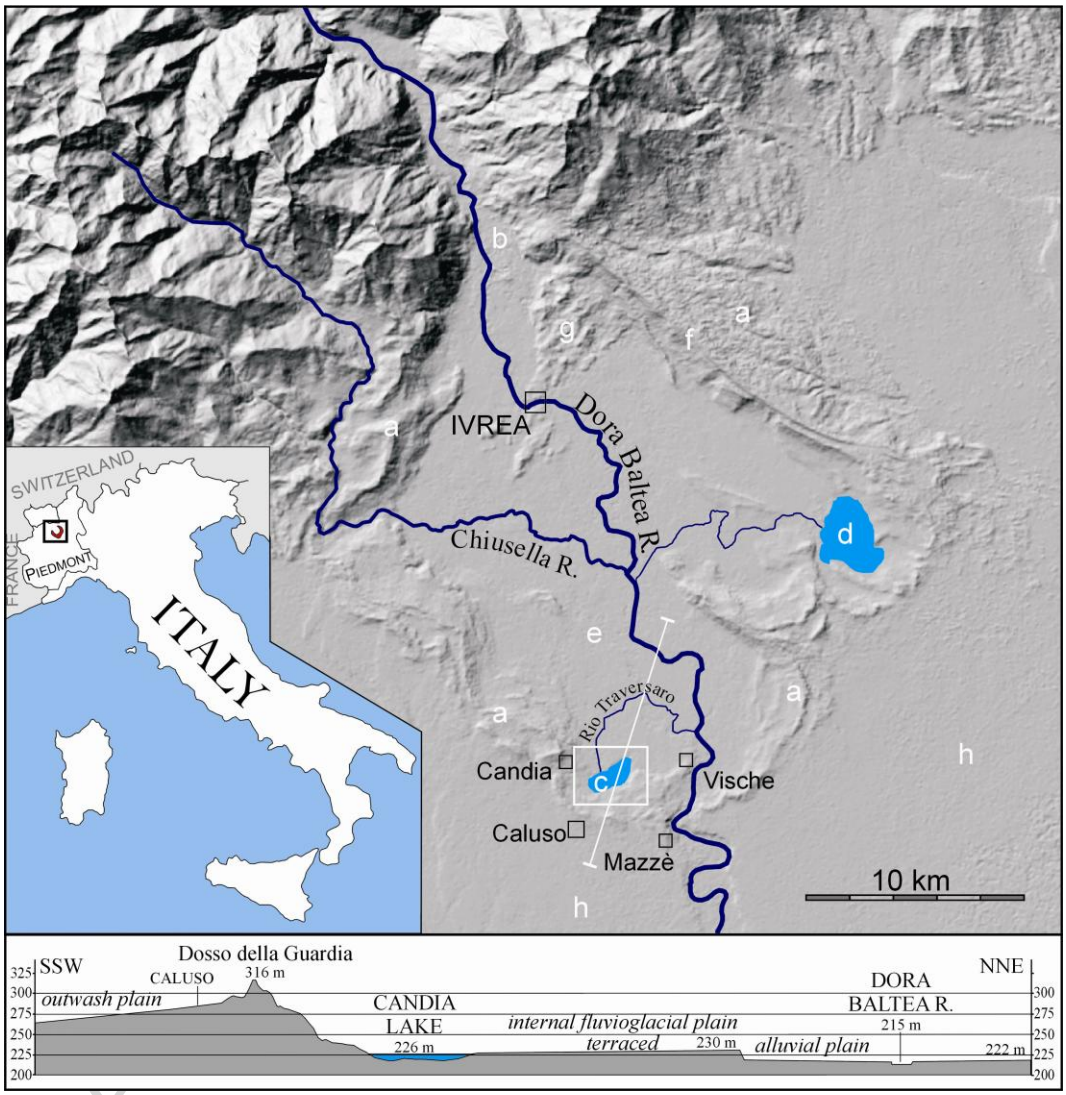

Figure 1

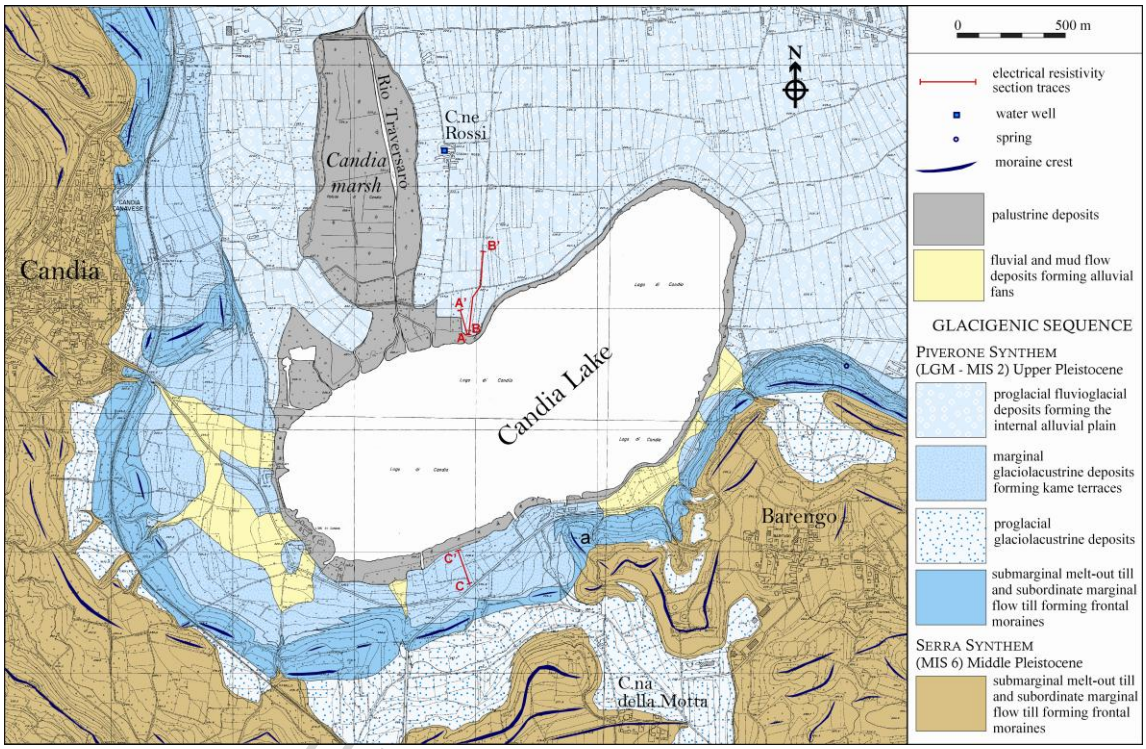

Figure 2

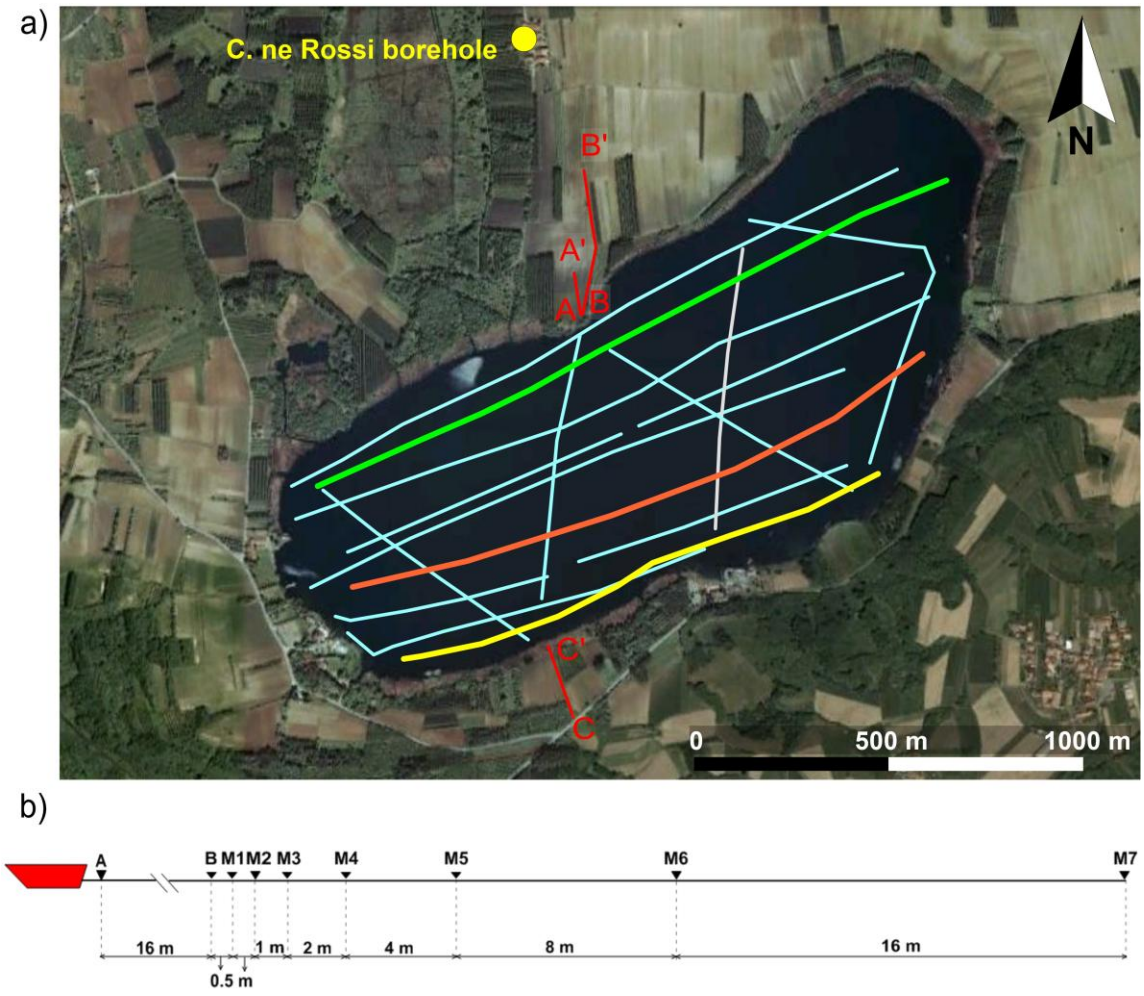

Figure 3

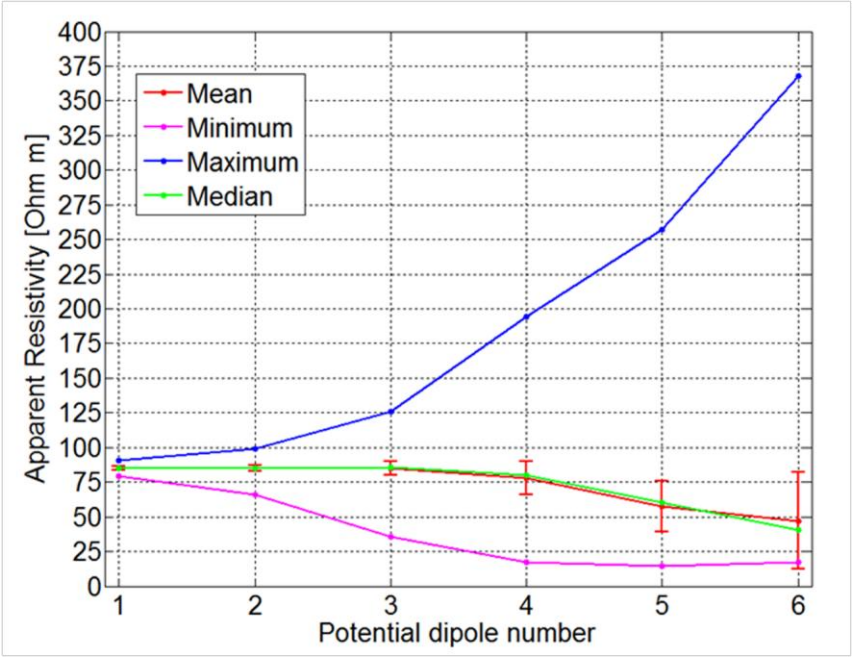

Figure 4

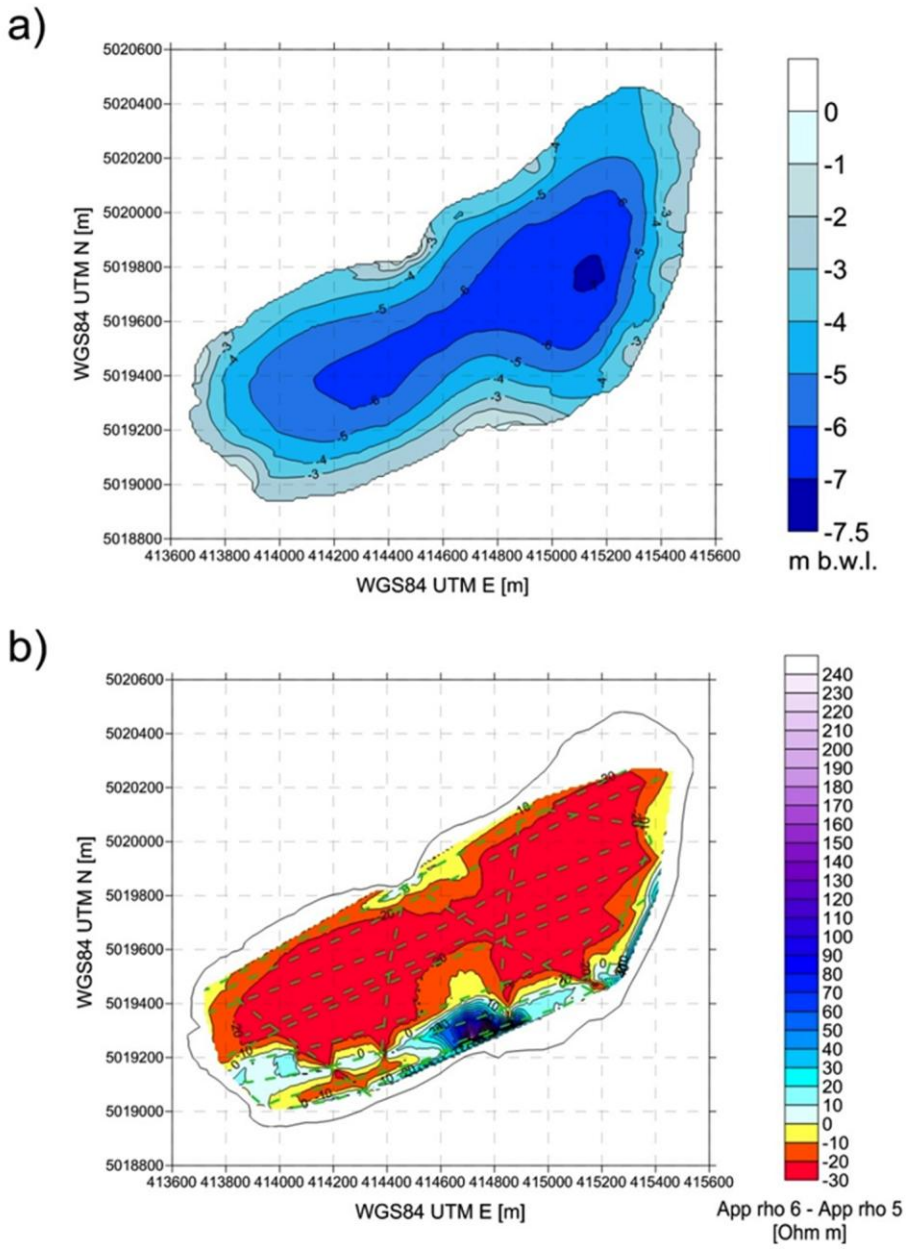
a)
WGS84 UTM N [m]
5020600
5020400
5020200
5020000
5019800
5019600
5019400
5019200
5019000
5018800
413600 413800 414000 414200 414400 414600 414800 415000 415200 415400 415600
WGS84 UTM E [m]
0
-1
-2
-3
-4
-5
-6
-7
-7.5
m b.w.l.
b)
WGS84 UTM N [m]
WGS84 UTM E [m]
240
230
220
210
200
190
180
170
160
150
140
130
120
110
100
90
80
70
60
50
40
30
20
10
0
-10
-20
-30
App rho 6 - App rho 5
[Ohm m]

Figure 5

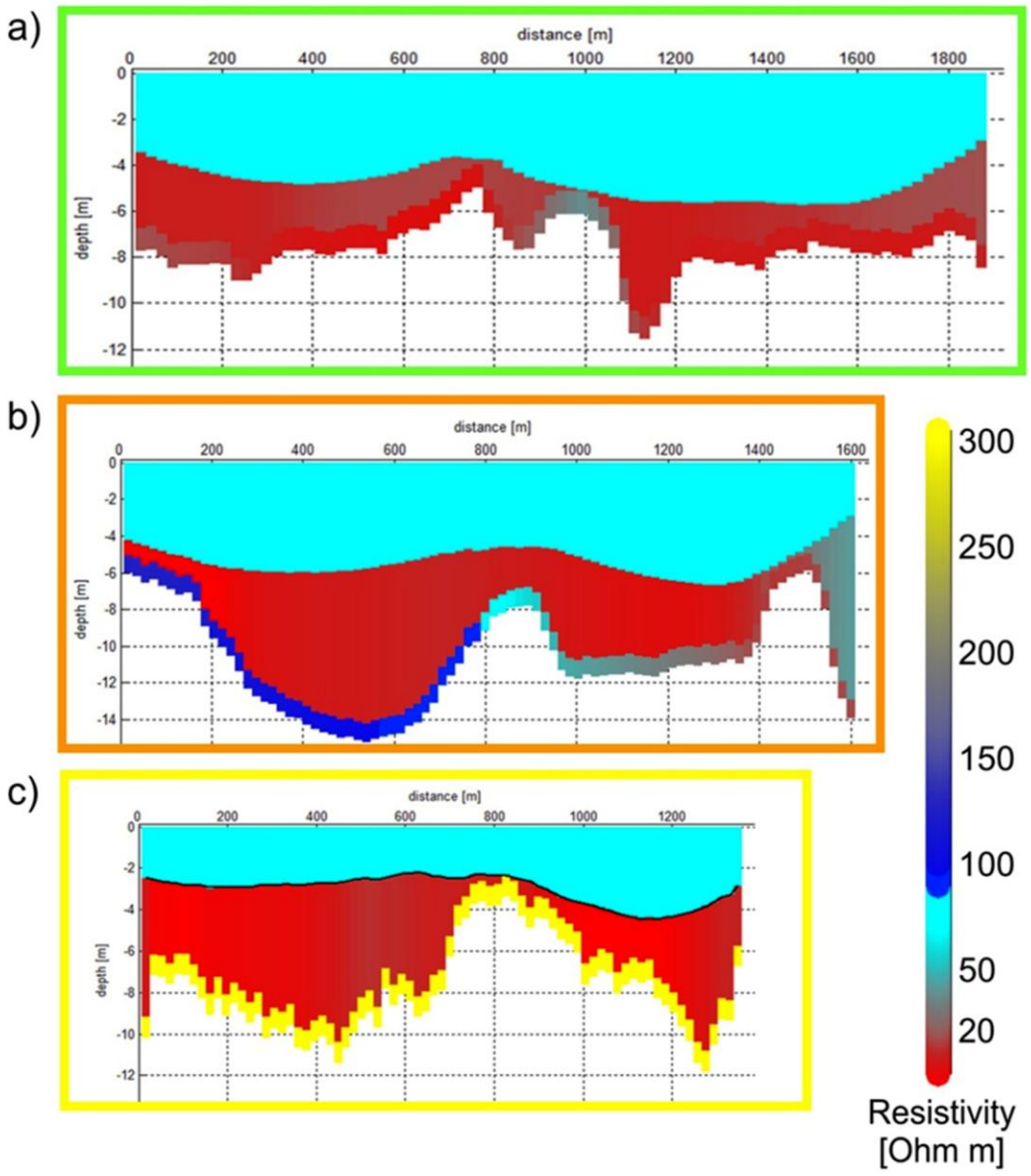

Figure 6

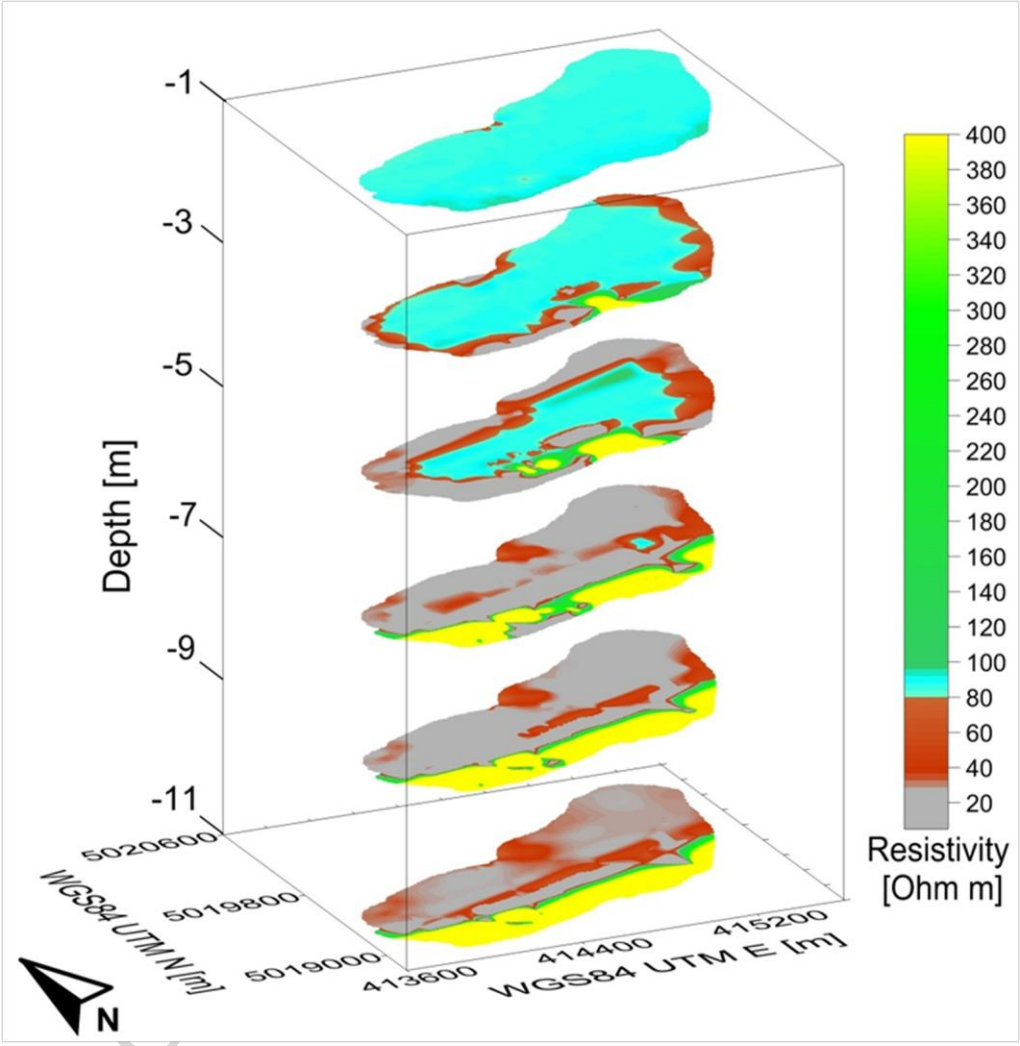

Figure 7

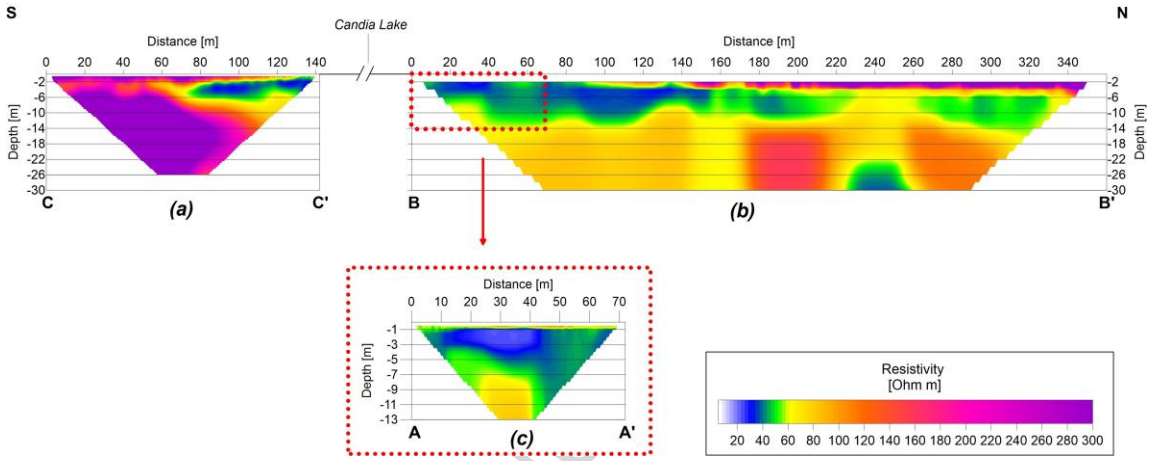

Figure 8

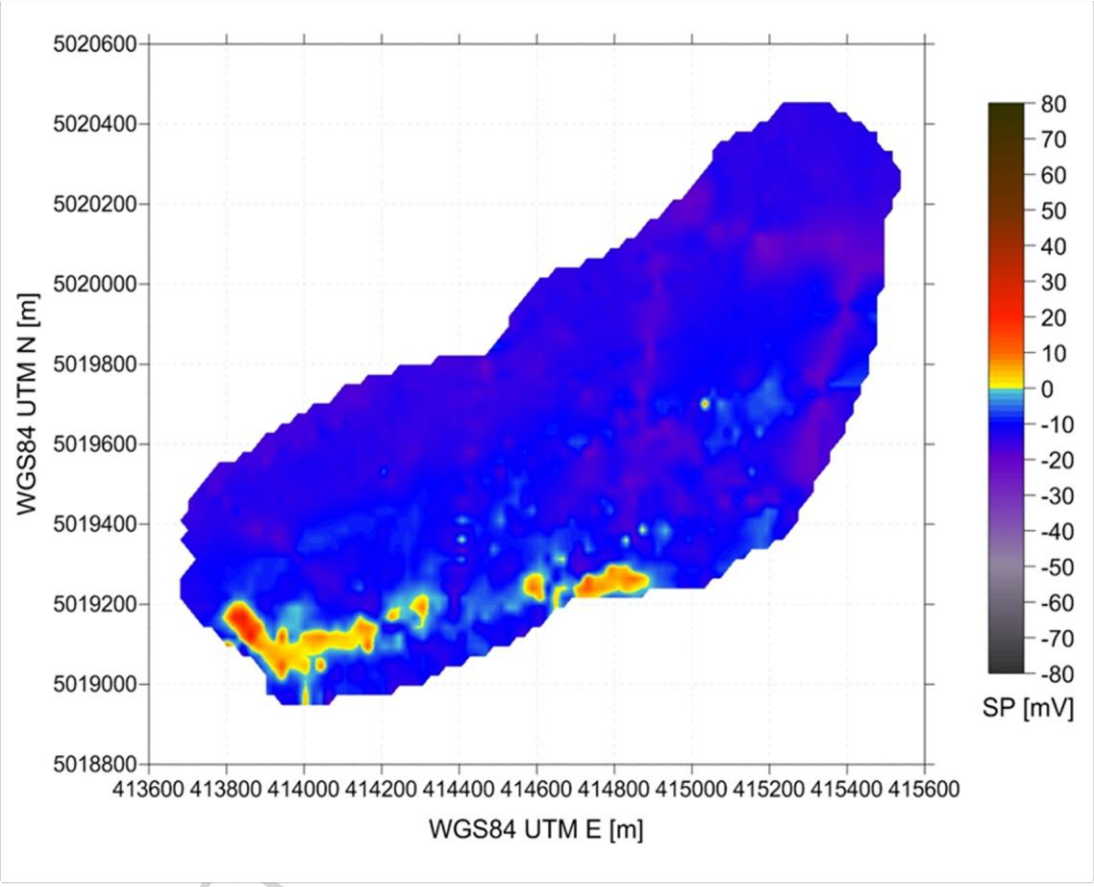

Figure 9

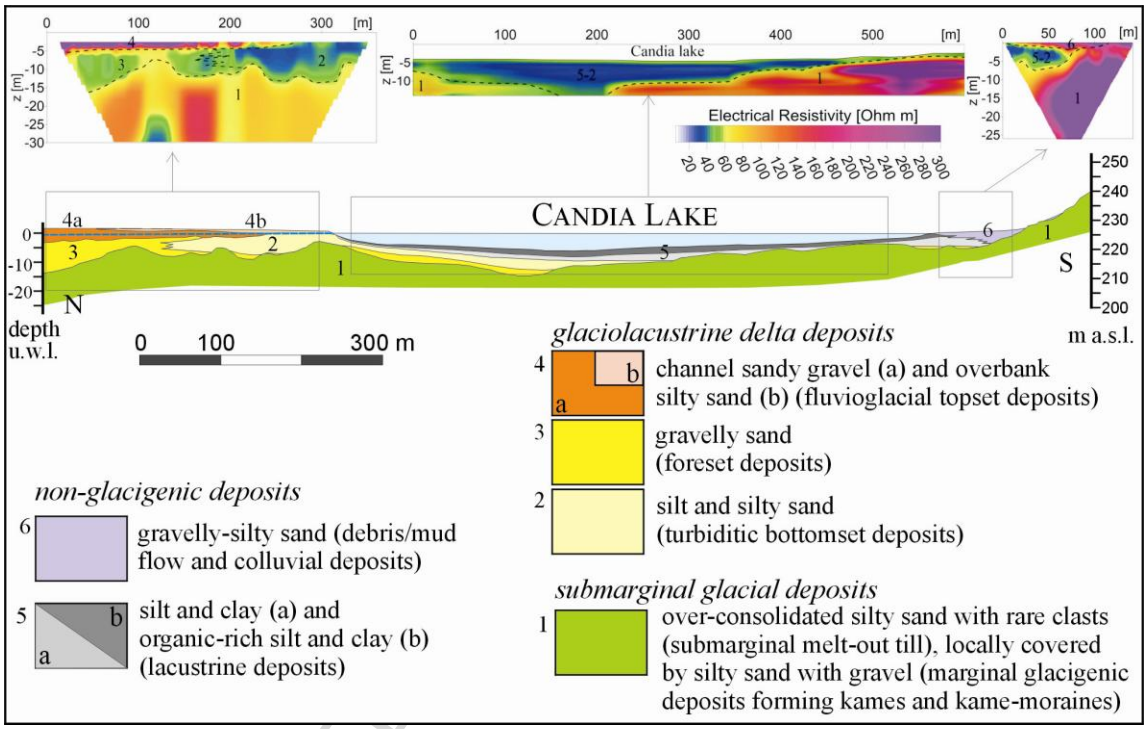

Figure 10

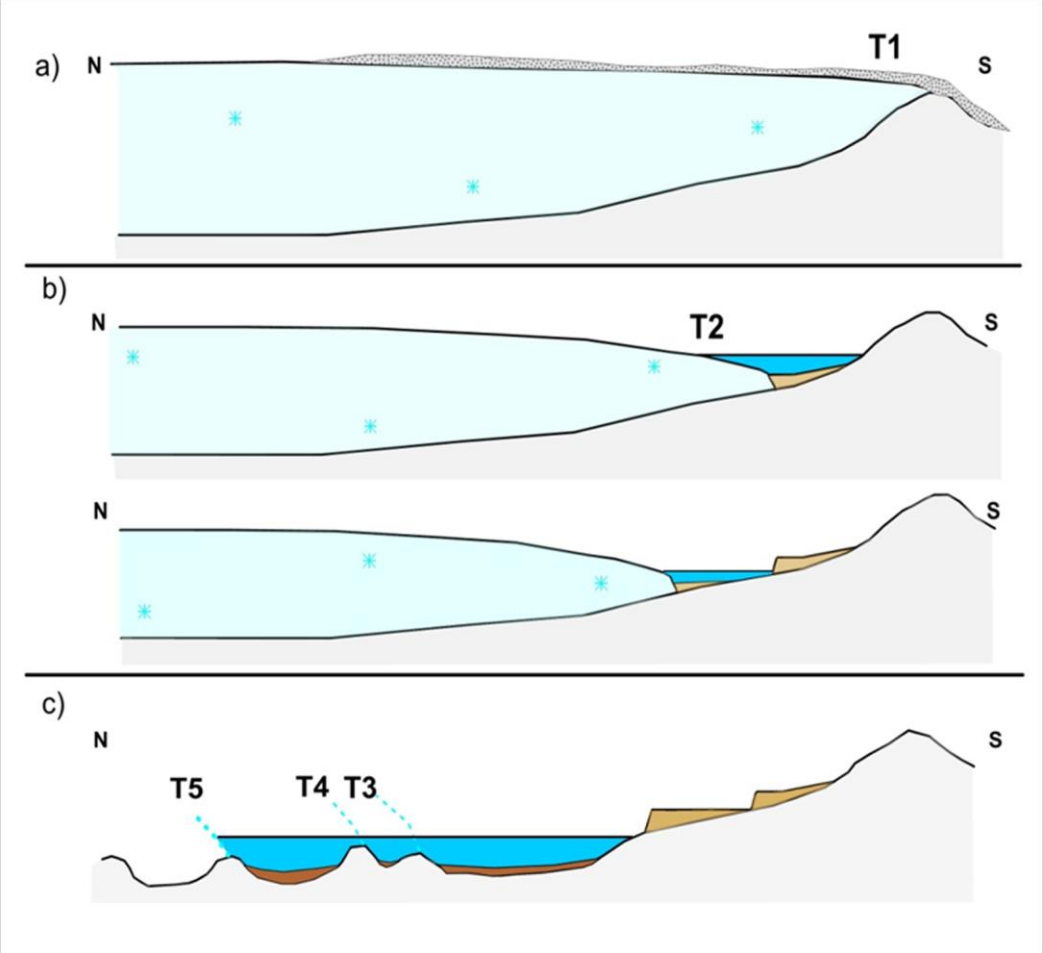

Figure 11

HIGHLIGHTS

(i) CVES for determining the stratigraphical setting of an underwater environment**;**

(ii) Multiple and combined use of on-land and off-shore resistivity data;

(iii) Definition of areas of groundwater recharge and lake basin genesis;